ECOHYDROLOGY
Ecohydrol. (2010)
Published online in Wiley Online Library
(wileyonlinelibrary.com) DOI: 10.1002/eco.178

A numerical study on hydrological impacts of forest restoration in the southern United States

Yongqiang Liu*
Center for Forest Disturbance Science, USDA Forest Service, Athens, GA 30602, USA

ABSTRACT

Landscape in the southern United States changed dramatically during the 1930s and the following decades when massive agricultural and abandoned logging lands were converted to forest lands through natural restoration and silviculture. The impacts of this forest restoration on hydrology were investigated in this study by conducting numerical experiments with a regional climate model. Climatic and hydrological conditions for the months of January and July during an 8-year period were simulated with prior and post forest conversion land cover, respectively. The assembled results of the simulations and experiments during the period indicate that overall precipitation decreases in July and increases in January in the restoration region (RR) in response to the restoration, mainly caused by the reduction in the corresponding prevailing winds due to increased surface roughness. Evapotranspiration and root-layer soil moisture increase in both months, mainly caused by the changes in vegetation and soil properties. Solar radiation increases due to smaller albedo, most of which is used to increase sensible heat. Large increases in July precipitation, evapotranspiration, and runoff in the remote central Midwest are found, resulting from the change in the large-scale atmospheric circulation. The implications of the results for the projected vegetation changes due to the climate change and the silviculture project in the Southeast in the future are discussed. Published 2010. This article is a US Government work and is in the public domain in the USA.

KEY WORDS forest restoration; hydrology; climate; regional modeling; southern United States

Received 7 February 2010; Accepted 7 October 2010

INTRODUCTION

The southern United States consists of 13 states from Texas to the Atlantic coast and from Florida to Virginia. This region comprises one of the most productive forested areas in the United States with approximately 200 million acres or 40% of the nation's forests in an area of just over half a billion acres or only 24% of the United States land area (SRFRR, 1996). Furthermore, southern forests are dynamic ecosystems characterized by rapid growth within a favorable climate. The forest ecosystems bring great environmental benefits such as water conservation and climate regulation to this region. Evapotranspiration from vegetated lands can reduce air temperature through latent heat consumption and transports water vapor into the atmosphere. This leads to an increase in air relative humidity, which often contributes to an increase in local precipitation.

Land cover in this region has changed dramatically in the last century (Sampson, 2004). The region's forest acreage declined in the 19th century and early 20th century and reached a low some time around 1920 as a result of agricultural land clearing and timber harvesting (USDAFS, 1988). This trend turned around in the 1930s, especially after the Great Depression, when massive agricultural and abandoned logging lands were converted to forest lands through planting trees on public and private lands as part of the nationwide forestry and land conservation programs which planted billions of trees.

Land-cover change at a regional scale such as the forest restoration in the southern United States can affect regional hydrologic and climatic conditions through changing the surface energy and water fluxes, soil hydraulic property, and surface roughness (Lean and Warrilow, 1989; Nobre *et al.*, 1991; Dickinson and Kennedy, 1992). Many studies have provided simulation and measurement evidence of the importance of land-cover change to regional hydrology (Pielke and Avissar, 1990; Shukla *et al.*, 1990; Dickinson *et al.*, 1993; Xue, 1996; Bonan, 1997; Liu *et al.*, 2008). Latent heat energy is necessary for evapotranspiration. When land cover is replaced with a different type of vegetation, surface albedo is changed and thus the solar radiation absorbed on the ground will be different. This will change latent heat energy and, therefore, evapotranspiration. Dickinson *et al.* (1993) found that deforestation of the Amazon basin would cause a decrease in evapotranspiration by about 20 mm per month. Roots of vegetation can promote soil porosity and prevent runoff. This is different from soil porosity change due to compaction, which can be caused by machine use during land-use activities. Total runoff would be reduced by about 20 mm per month in the Amazon deforestation (Dickinson *et al.*, 1993). Vegetated surface has larger roughness than bared soil, leading

* Correspondence to: Yongqiang Liu, Center for Forest Disturbance Science, USDA Forest Service, 320 Green St., Athens, GA 30602, USA. E-mail: yliu@fs.fed.us

to stronger turbulence. As a result, water vapor and heat exchanges on the land surface become larger.

The Amazon region has attracted early attention because of the extensive deforestation and the potentially significant hydrologic and climatic impacts. Such impacts could be expected in the southern United States due to some similarities in the land–atmosphere interactions between the two regions. The variability in a land–atmosphere coupled system results from two types of processes: internal ones through local exchanges of energy, momentum, heat, water, and other gases and particles between the atmosphere and land surface, and external ones through horizontal transports of these properties by the atmospheric circulation. Despite the different magnitude in the air–land exchanges duo to the differences in vegetation and soil types, the two regions have common internal processes. The external processes are region dependent because prevailing atmospheric circulation systems may change from one region to another. However, both regions are located in the tropical or subtropical areas and are controlled by the subtropical high pressure systems during warm seasons. Thus, the southern United States is likely comparable to the Amazon in the hydrologic and climatic impacts of landscape change. This is different from a large-scale forest restoration program in northern China (Liu *et al.*, 2008), which is located in the mid-latitudes and controlled mainly by the westerly atmospheric systems. There are many factors for the relative importance between the two types of processes in a specific region. First, normally the larger the size of the land-cover change, the more important the internal processes. Second, the land–atmosphere interactions are stronger under warm conditions than cool ones because of the more intensive land–atmosphere interaction. Thus, it is expected that the impacts of land-cover change on local and regional hydrology in the Amazon, which is larger in size and warmer, are more significant than in the southern United States.

McVicar *et al.* (2007) pointed out the positive hydrological impacts of the afforestation in the Loess Plateau of Northwest China, including a reduction in erosion and the risk of average flooding. A counter to the positive impacts is the often observed reduction in streamflow (Jackson *et al.*, 2005; Sun *et al.*, 2006), largely due to increasing rates of evapotranspiration. Jackson *et al.* (2005) analyzed catchment observations from different world regions and found that afforestation dramatically decreased streamflow within a few years of planting. They projected the impacts of different plantation scenarios in the eastern United States using the Forest and Agricultural Sector Optimization Model–Greenhouse Gases (FASOMGHG). Farmlands at some spot locations along the Gulf and southern Atlantic coast will be changed to evergreen needleleaf forest and large areas of farmlands in the Midwest will be changed to deciduous broadleaf or evergreen needleleaf forest. They further projected the atmospheric response with the Regional Atmospheric Modeling System (RAMS). The potential changes include dominated evapotranspiration increase and precipitation decrease in response to the plantations.

Land cover will change significantly in the future due to climate change and silviculture. Many global general circulation models (GCMs) have projected significant climate change by the end of this century due to the greenhouse effect, including warming and drying trends in many subtropical and mid-latitude regions (IPCC, 2007). This will lead to changes in land cover. For example, a modeling study projected that a large portion of the temperate deciduous forests in the Southeast would be replaced with temperate deciduous savanna in response to the projected climate change (Neilson *et al.*, 1998, 2005). Meanwhile, there is a plan to plant about 18 million acres of new trees to replace pasture and farming lands by 2020 in the United States (Watson, 2009). The afforestation project would be even larger than the one carried out by the Civilian Conservation Corps during the Great Depression, which planted 3 billion trees from 1933 to 1942.

This study conducts numerical experiments with a regional climate model on the response of hydrological conditions to land-cover change similar to the farming-forest conversion in the southern United States during the 1930s. In contrast to the actual conversion processes that took decades, this study assumes instant conversion without plant growth involved in the simulation, an approach applied in many studies on trends of hydrological variations in responses to land-cover change, including the one we did for the northern China forest restoration program (Liu *et al.*, 2008). It helps to understand the short-term responses of the atmosphere and soil surface and root layers at daily, monthly, and seasonal scales to land-cover changes. Study findings will provide useful information on the importance of forest restoration to historical local and regional climatic and hydrological variability and on implications for possible hydrological response to the projected replacement of temperate deciduous forest with deciduous savanna due to the climate change and planned silviculture in the future. The future US silviculture project (Watson, 2009) plans to plant trees in the Southeast, Great Lake states and the Corn Belt states. The hydrologic impacts of the project are expected to be different among these regions, and even in different areas within one region. In addition, the silviculture of a region can affect hydrologic conditions outside the region. This study will investigate the historical silviculture in the southern United States and compare it with a silviculture project in the mid-latitude region. The results will help understand the geographic dependence of silviculture and select the areas for tree planting where possibly best hydrologic and climatic outcomes could be expected.

METHODS

Conceptual model

Figure 1 shows various physical processes through which forest restoration affects climate and hydrology. These happen at both the local scale within a restored region

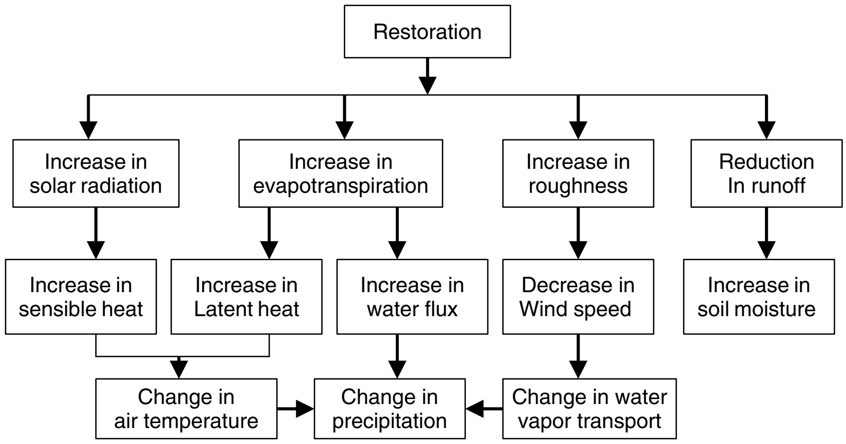

Figure 1. A conceptual model of the impacts of restoration on climate and hydrology.

through changing energy, heat, and water fluxes on the land surface, and the regional scale over the region and its surrounding areas through changing atmospheric circulation. Forested lands have smaller albedo, larger transpiration rates, roughness, and water capacity than farming lands. Smaller surface albedo leads to more solar radiative energy absorbed on the ground, which is converted into larger sensible and latent heat fluxes and air temperature change. Larger transpiration moves soil water in the root layer into the atmosphere through leaf stomata. Larger roughness reduces prevailing wind speeds on the ground and therefore changes water vapor transport in the atmosphere. Greater holding capacity of soil moisture contributes to runoff reduction. Precipitation, determined by water vapor availability, vertical velocity, and thermal instability, is modified in response to the changes in temperature and vertical and horizontal water transports.

Numerical model

A regional climate model (RCM) was used to simulate atmospheric and soil conditions and their changes. An RCM is constructed based on a limited-area weather model (LAM). RCMs usually include more detailed descriptions of some physical processes important to climate, including radiation, land-surface, planetary-boundary-layer, and precipitation. These processes are very simple or not included in a weather model because they may not be very important for short-term atmospheric variations. The lateral boundary conditions of RCM simulations are provided by either GCM simulations or actual measurements. The regional climate modeling technique was first developed in the late 1980s in the US National Center for Atmospheric Research (NCAR) based on the standard NCAR/Penn State Mesoscale Model Version 4 (MM4) (Anthes *et al.*, 1987; Dickinson *et al.*, 1989; Giorgi and Bates, 1989). Many RCMs have been developed since then based on other LAMs, including the National Centers for Environmental Prediction (NCEP) regional spectral model (RSM) (Juang and Kanamitsu, 1994), the Hadley Centre regional climate modeling system (Jones *et al.*, 1995), the Canadian regional climate model (CRCM) (Caya and Laprise, 1999), the climate version of the Colorado State University RAMS (Liston and Pielke, 2000), and the climate version of the weather research and forecast (WRF) model (Liang *et al.*, 2006), which was developed based on NCAR/Penn State Mesoscale Model Version 5 (MM5).

RCMs can address some of the scale issues associated with applications of low-resolution GCMs to regional climate modeling. GCMs have limited capacity to simulate regional scale climate and mesoscale processes such as convective storms because their resolution is mostly at several hundred kilometers. The effects of local and regional forcing such as terrain, land cover variability, and aerosols emitted from natural and anthropogenic sources are often not well represented in GCMs. RCMs, on the other hand, have spatial resolution at tens of kilometers or higher and are often equipped with more detailed schemes for local and regional properties, thereby providing a better tool for understanding climate at regional scale. Unlike GCMs, which can be run as long as thousands of years, RCMs usually are run from months to years because of extreme computer time consumption due to high resolution and more detailed description of physical processes. In contrast to GCMS, which are mostly spectral models, RCMs are mostly grid-point models.

However, there are some limitations to the RCM modeling technique (Liu, 2007). First of all, RCMs are driven by GCMs and/or measurements; any errors in lateral conditions will be passed to RCMs. Experiments have indicated large sensitivity of RCM simulations to lateral conditions. Even though a complex local land-surface condition was one of the reasons for using RCMs, information deficiencies limit the ability of RCMs to reproduce important features in the atmosphere and other earth components. Soil moisture and snow are among the data elements for which very little information is available in some areas. This could lead to errors in simulation of soil moisture, albedo, and evapotranspiration. This limitation, however, would have very limited impacts on this study because of the focus on the differences between two types of simulations with agriculture and forest land covers, as described below, and almost no snow in the region of land-cover change in the southern United States. In addition, domain size and internal variability created by disturbances in initial and boundary conditions also affect RCM performance (Seth and Giorgi, 1998; Giorgi and Bi, 2000).

The NCAR regional climate model (RegCM) (Giorgi *et al.*, 1993a,b) with modified explicit rainfall calculation (Giorgi and Shields, 1999) was used to conduct regional climate modeling. RegCM characterizes regional features of the climate by incorporating biosphere–atmosphere transfer scheme (BATS) land-surface physics (Dickinson *et al.*, 1995) and the NCAR radiative transfer model (Kiehl *et al.*, 1996), into the standard NCAR/Penn State Mesoscale Model (Anthes *et al.*, 1987). RegCM is able to reproduce some important high-resolution spatial characteristics of the climate for major geographic regions over the world.

BATS has three soil layers (the surface, root zone, and a third layer between the root zone and the groundwater layer), extending from the soil surface to 0·1 m, 1 or 2 m (depending upon land cover type), and 3 m, respectively. Soil moisture of each layer varies mainly as a result of precipitation, evapotranspiration, and runoff. Soil moisture is also determined by soil-vegetation water exchanges through root absorption in the root zone and water exchange with the groundwater layer in the third layer. The water level of the groundwater layer is assumed to be constant, despite the finding that the water level could fluctuate remarkably during a prolonged drought event such as the 2003 European drought (Andersen *et al.*, 2005). The possible fluctuation would have limited impacts on this study because the period of each simulation was only 1-month long and severe drought was observed only for one simulation (July 1988) (see below for a description of simulations).

The evaporation portion of evapotranspiration in BATS is measured by either potential evaporation or maximum moisture flux through the wet surface that the soil can sustain, whichever is smaller. Potential evaporation is proportional to the difference between saturated air specific humidity at the surface and air specific humidity at the lowest model level, wind speed, and drag coefficient or resistance. The last parameter is a function of atmospheric stability, vegetation type, and coverage. Maximum moisture flux is determined mainly by soil moisture and a soil parameter depending on soil texture which defines change in soil water potential and hydraulic conductivity with soil water. The transpiration portion of evapotranspiration is related to stomatal resistance, which is a function of radiation, vapor pressure deficit, soil moisture, and temperature. Runoff is proportional to precipitation linearly, and relative soil moisture (the ratio of actual soil water to soil water capacity) to the power of four.

Simulations

The simulation domain covers the continental United States (Figure 2). The topography is characterized by

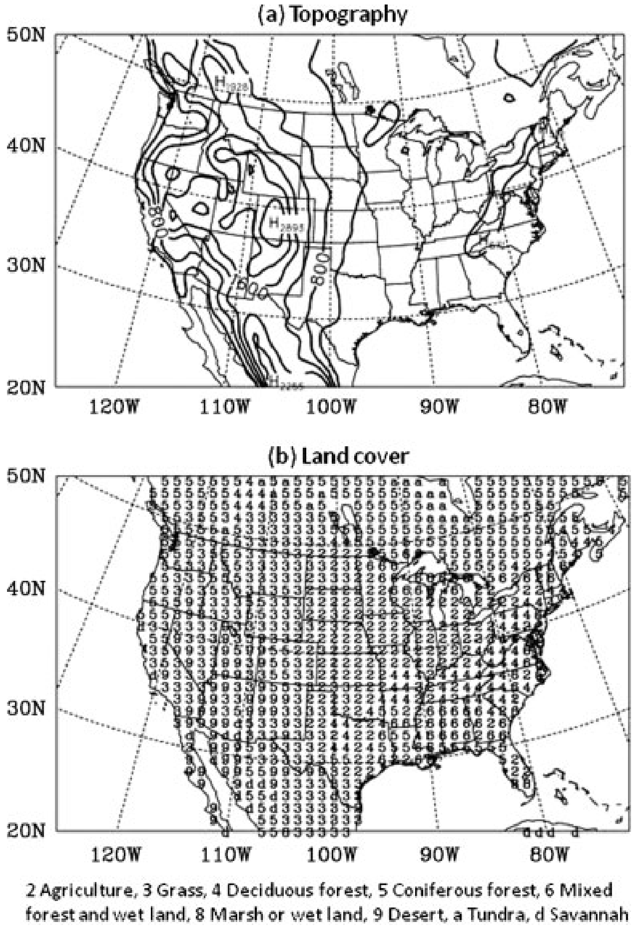

Figure 2. Simulation domain. (a) Topography with contour interval of 400 m. (b) Land cover with legend shown below the figure.

mountains in the west and flat lands in the east. The dominant land cover types in the South include deciduous forest, coniferous forest, and mixed forest and wet land. Agricultural lands are found in the Mississippi River basin, eastern Texas, as well as some spots along the Atlantic coast. The dominant land cover types in other regions include coniferous forest and grass in the Northwest, coniferous forest, grass, and desert in the Southwest, agriculture in the Midwest, and deciduous forest in the Northeast. The domain is centered at 40 °N and 99 °W and contains 97 × 61 grid points with a horizontal resolution of 60 km. There are 14 vertical layers with the top model atmosphere at 80 hPa. There are two types of precipitation, non-convective and convective. The former is formed when the atmosphere is saturated and is usually related to large-scale weather systems such as fronts. The model decides the formation of non-convective precipitation based on the simulated air humidity. The latter, on the other hand, is formed with intense upward motion of the air mass and has a size often smaller than the model grid size. Thus, it cannot be decided directly based on the simulated variables. Instead, a technique called convective parameterization is used. The Grell sub-grid convective scheme (Grell *et al.*, 1994) was utilized for this study.

A total of 32 simulations were conducted, each for one of the 8-year period from 1988 to 1995, a winter or summer month, and an agriculture or forest land cover in the restoration region (RR). The 8-year period included an extreme drought event in 1988, an extreme flood event in 1993, and mostly normal weather conditions in other years in the northern United States The ensemble of these simulations was analyzed for all hydrological components, while precipitation was also analyzed for individual years. January and July were used to represent winter and summer conditions, respectively. Despite certain differences between monthly and seasonal meteorological conditions, the 2 months are often used to represent winter and summer conditions, respectively. The general climate patterns of the two seasons will be described in the Section on Results. The two land cover cases will be described later.

The initial and horizontal lateral boundary conditions for the RegCM simulations of wind, temperature, water vapor, and surface pressure were interpolated from the analysis of the European Center for Medium-Range Weather Forecast (ECMWF), whose resolution is 1·875° of latitude and longitude (roughly 200 × 175 km at mid-latitudes). Soil water content was initialized using a technique described by Giorgi and Bates (1989), It was equal to the sum of wilting soil moisture, at which transpiration ceases, and the difference between saturation and wilting soil moisture weighted by soil moisture availability, which is specified for each surface type. Because soil moisture is not a regular measured property, parameterization schemes like the one used for RegCM have to be used. It is one of the limitations in meteorological modeling coupled with land-surface processes, though its impact on surface-layer soil moisture is not significant because it adjusts fast through rapid interactions with the atmospheric processes. An assimilation approach that determines initial soil moisture using historical precipitation and other information has been developed, but has yet to be applied in RegCM. Time-dependent sea-surface temperature (SST) was interpolated from a set of observed, monthly mean with a resolution of 1° (Shea *et al.*, 1992). All these data were obtained from archives of the NCAR Scientific Computing Division. Land type was specified based on the global 1-km resolution International Geosphere Biosphere Program (IGBP) land cover data set (Zeng *et al.*, 2000).

The meteorological data for these years were originally collected in a previous study on the climate effects of atmospheric aerosols in the United States (Liu *et al.*, 2000). They have also been used to understand climate and wildfire interactions, including the impacts of the 1988 Yellowstone National Park wildfire on the northern US drought, wildfire potential evaluation, and future wildfire potential projection (Liu, 2005; Liu *et al.*, 2010a, 2010b). These investigations indicated that spatial patterns of precipitation and temperature simulated with RegCM agreed with the observed conditions.

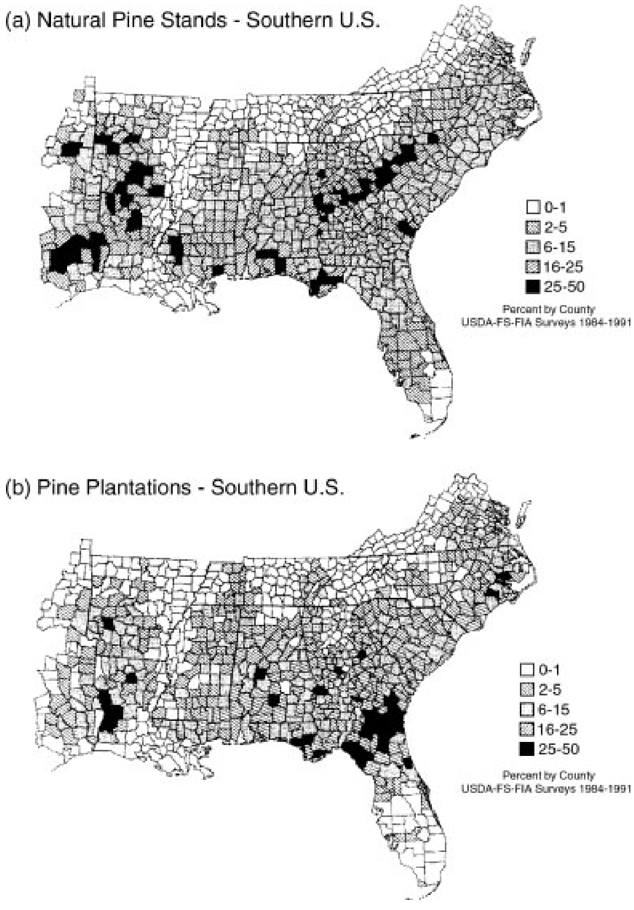

Figure 3. Percentage of southeastern counties in natural pine stands (a) and pine plantations (b) (from Allen *et al.*, 1996).

Restoration specification

The land-cover change related to the forest restoration in the South was specified based on the forest monitoring data illustrated in Figure 3 (Allen *et al.*, 1996). The forest restoration occurred through natural restoration and plantation. Natural pine forests dominated along the southern Piedmont, selected counties on the southern coastal plain and upland areas west of the Mississippi River. Pine plantations dominated in northern Florida and other counties throughout the coastal plain. This historical data has different features from the projected future plantations with FASOMGHG (Jackson *et al.*, 2005). First, the forest coverage change during the conversion period occurred not only through plantation but also natural restoration and other restoration approach (Stanturf *et al.*, 2000). Second, the land-cover change was limited in the southern region, but happened in more extensive areas.

Simulations using two types of land cover, denoted as AGRI and FOREST, were conducted for January and July over the 8-year periods. Land cover in AGRI and FOREST was the same in the entire simulation domain except an RR (Figure 4). This region, about 1·33 million km^2, was covered with agricultural lands in AGRI, but about 70% of the region (0·93 million km^2) was replaced with trees in FOREST. The replacement locations were specified based on the monitoring data described above

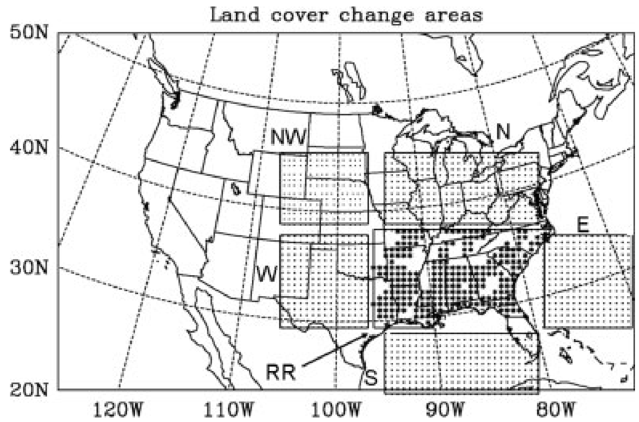

Figure 4. Forest restoration region (RR) indicated by asterisks in the central area and surrounding areas indicated by dots in north (N), northwest (NW), west (W), south (S), and east (E).

(Allen *et al*., 1996). FOREST was used to represent post-restoration conditions, while the differences between FOREST and AGRI represent the changes due to the forest restoration.

Evaluation

The major forest restoration activities related to the conversion of farming to forest land occurred in the late 1930s after the Great Depression. The observed January and July precipitation and air temperature were averaged over the 1930s (1930–1939) and the 1940s (1940–1949) to represent the prior and post-meteorological conditions, respectively. The differences between the 1940s and 1930s were used to see if the restoration might have actually contributed to the realistic atmospheric variability.

RESULTS AND DISCUSSION

Restoration area

Precipitation. Figure 5 shows the assembling of present precipitation (FOREST) and the change due to the forest restoration (the difference between FOREST and AGRI). Present January precipitation occurs in two regions. One is the eastern United States with rainfall of about 160 mm off the southern Atlantic coast. The RR, located west of the precipitation center, has rainfall of about 120 mm. The other is the northwestern Pacific coast with the same intensity. July precipitation is also large in the eastern United States Its center is moved to the inland area from its January location in the ocean area. Rainfall is about twice as large as the January amount. Rainfall decreases from about 300 mm in the northeastern portion of the RR, which is within the major rainfall region, to about 160 mm in the southwestern portion. Rainfall is relatively small in the western United States, less than 40 mm along the Pacific coast.

To analyze precipitation and other properties more quantitatively, the average was calculated over the model grids within the RR. It was also calculated for three surrounding land areas in north (N), northwest (NW) and west (W), and two ocean or mostly ocean ones in the south (S) and east (E) (refer Figure 4 for their locations). Rainfall averages in RR are 107 mm in January and 213 mm in July (Table I).

Changes in January precipitation due to the forest restoration are found to be negative from the Louisiana (LA) coast to the northern RR and further to the Northeast, but positive in northern LA and from northern Georgia (GA) to the mid-Atlantic coast. The magnitude

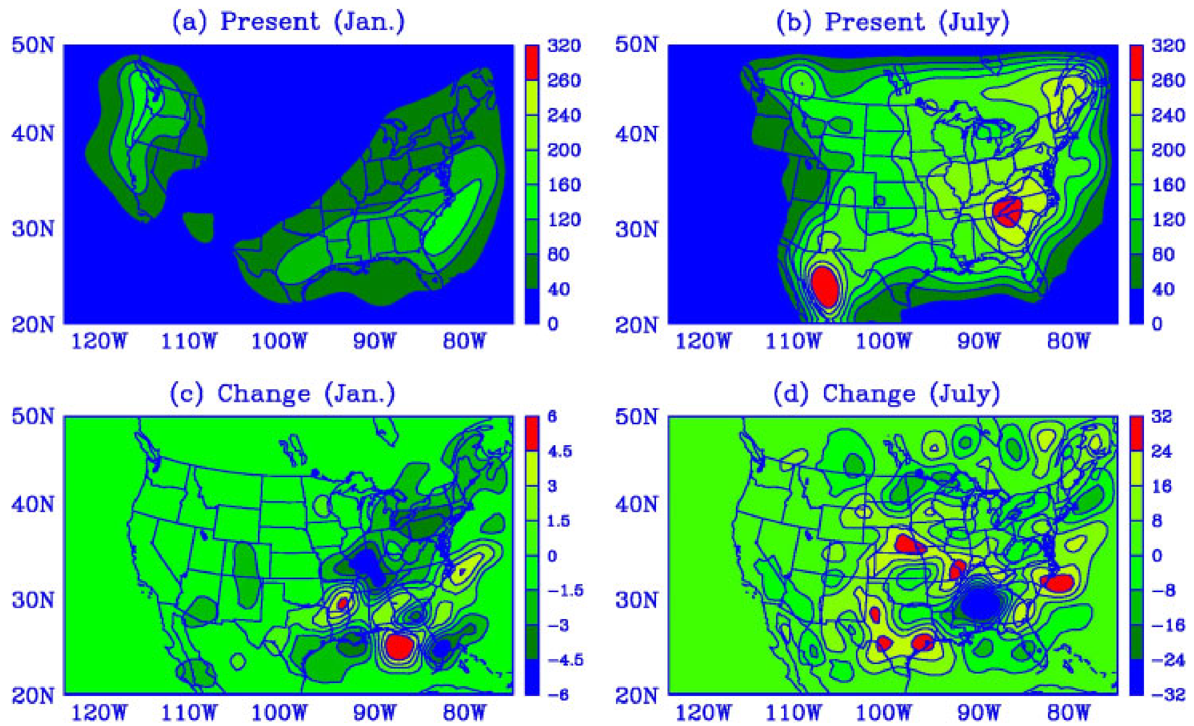

Figure 5. Precipitation (mm/months) averaged over 8 years for present precipitation in January (a) and July (b), and change due to forest restoration in January (c) and July (d).

Table I. Water fluxes (mm/months) for the restoration region (RR), north (N), northwest (NW), west (W), south (S) and east (E) areas.

Area	Precipitation		Evapotranspiration		Runoff	
	January	July	January	July	January	July
RR	107 (0·3)	213 (−1·9)	45 (0·3)	185 (1·5)	28 (5·6)	49 (7·7)
N	68 (−1·0)	209 (1·7)	18 (0·3)	174 (3·1)	15 (1·5)	41 (4·7)
NW	20 (0·1)	143 (9·8)	15 (1·0)	165 (12·7)	3 (0·6)	26 (5·8)
W	59 (0·2)	149 (4·7)	35 (1·5)	164 (9·8)	13 (2·2)	27 (3·5)
S	58 (0·8)	84 (−2·6)	148 (−3·5)	132 (−0·3)		
E	102 (0·7)	76 (2·7)	211 (−0·5)	113 (0·2)		

See Figure 4 for locations.

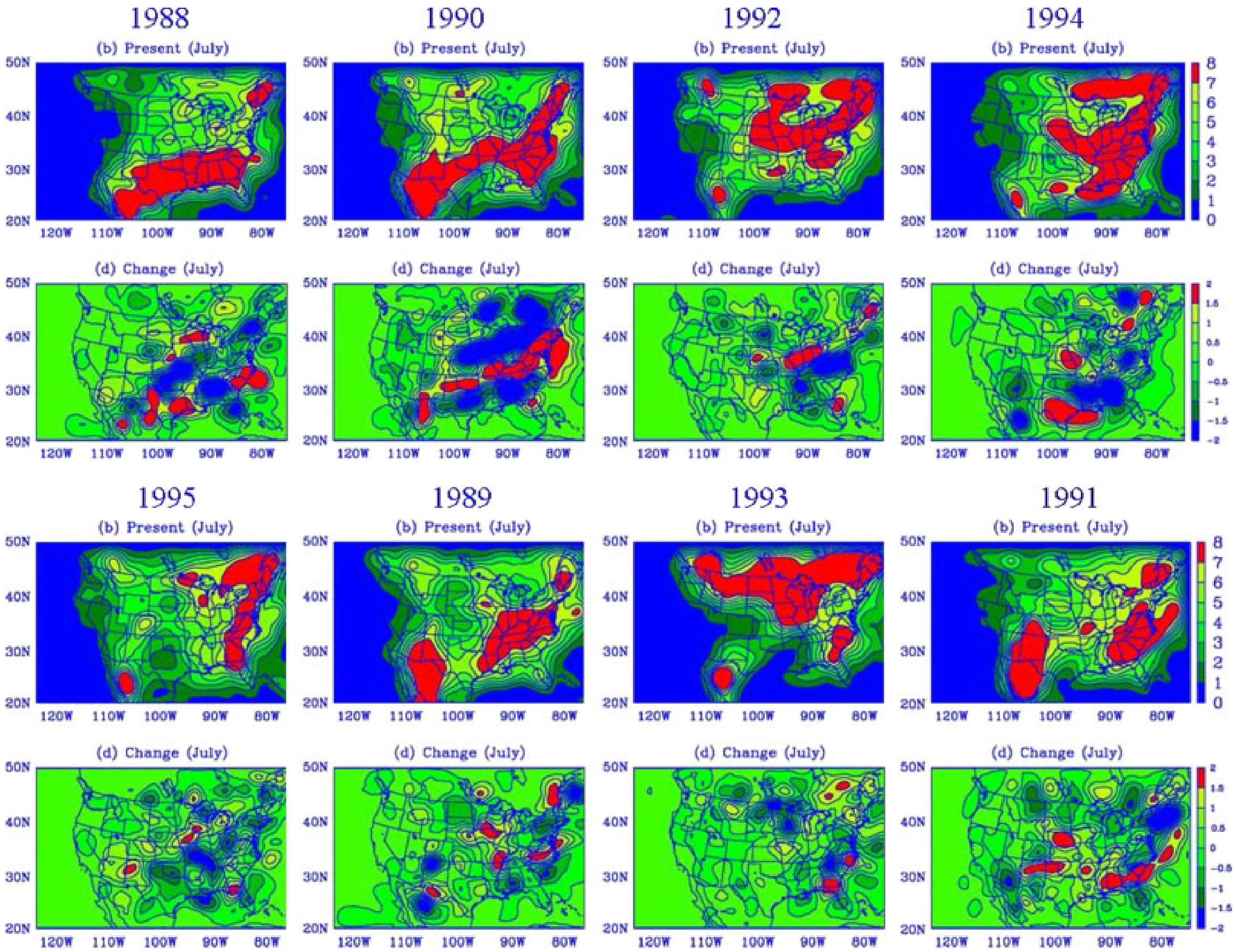

Figure 6. July precipitation (mm/months) of individual years. The top and bottom panels for each year are present precipitation and change due to forest restoration.

of the changes is 5 mm. Changes in July are negative, with a magnitude of 30 mm in the middle of the RR, slightly negative to the west, and positive in the Atlantic coast. Averages of rainfall change in RR are 0·3 mm in January and −1·9 mm in July (Table I). The change in winds could contribute to the change in precipitation. It is discussed later in the subsection on physical processes that the prevailing northerly cool and dry airflows in January are reduced in the RR, indicating that more water vapor is transported into the RR and there is therefore more precipitation. On the other hand, the prevailing warm and moist wind speed in July is reduced, indicating that less water vapor is transported into the RR and therefore there is less precipitation.

Figure 6 shows inter-annual variability of precipitation and its change. Two major features can be found. First, the spatial patterns of precipitation change have patchy structure with mixed signs. Precipitation is generated by weather systems such as fronts. Forest restoration can affect not only their intensity but also locations. If a weather system is forced to shift northward, e.g. precipitation would likely decrease at its original location, but increase in north. Also, total atmospheric water vapor transported from the ocean to land areas should

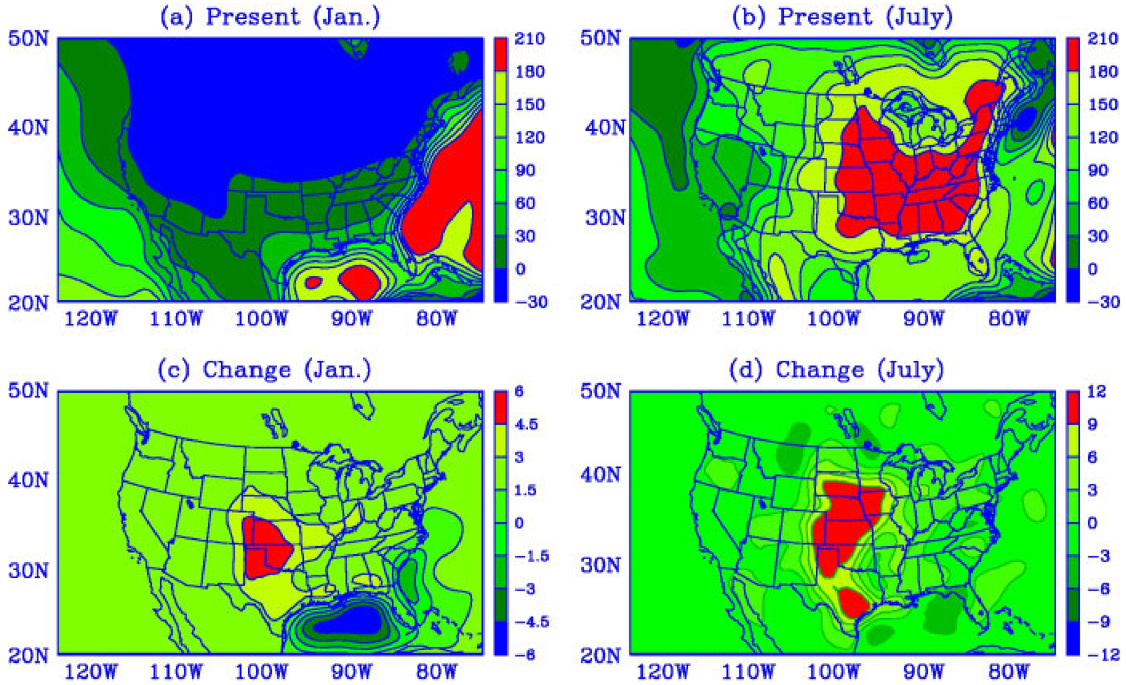

Figure 7. Evapotranspiration (mm/months) averaged over 8 years for present precipitation in January (a) and July (b), and change due to forest restoration in January (c) and July (d).

be conserved. If water vapor transported into the RR is reduced, that to its surrounding regions will be increased.

Second, the spatial patterns of precipitation change can be divided into three groups: (1) precipitation is remarkably reduced in most of the RR and surrounding areas, (2) precipitation is reduced in most of the RR but with small magnitude, and (3) precipitation mainly increases in the RR. Group 1 includes 5 years, i.e. 1988, 1990, 1992, 1994, and 1995. In 1988, precipitation decreases extensively in the Southeast and from southern Plains to the Northeast. Meanwhile, precipitation increases in some spots of southern Texas, mid-Atlantic coast, and the Great Lakes area. In 1990, there are two bands of reduced precipitation along the Gulf coast and the northern United States In between is a band of increased precipitation. Large precipitation reduction in 1992 is found in the northern RR and its surrounding areas. The spatial distribution in 1994 is similar to that in 1988. And precipitation reduction is dominant in 1995. Group 2 includes 1989 and 1993, and Group 3 has only one case of 1991. Atmospheric inter-annual variability should be responsible for the various groups of precipitation change. The specific mechanisms, however, have yet to be understood.

It appears that none of the groups is related to a particular pattern of average precipitation. Major average precipitation occurs in the southern United States (1988 and 1990), the northern United States (1992), the central as well as northern and southern United States (1994), and the Atlantic coast (1995) for Group 1, and in the Southeast (1989) and the northern United States (1993) for Group 2. The water vapor from the ocean areas is transported to the eastern United States, where major precipitation is found every year, and to the southwestern United States, where large precipitation is found for certain years. In one case each from Group 2 and Group 3, very large precipitation is found in the southwestern United States, probably indicating that more water vapor is transported to this region and less to the eastern United States than under normal conditions. Accordingly, the magnitude of overall water vapor transport decrease due to the restoration is larger in the southwestern United States and smaller in the eastern United States. As a result, the amount of reduction in the RR, which is within the major precipitation regime in the eastern United States, is smaller in certain areas for the two cases.

Evapotranspiration and runoff. The spatial patterns of average evapotranspiration (Figure 7) are different between January and July. Evapotranspiration consists of both evaporation and transpiration in land areas but only evaporation in ocean areas. January evapotranspiration is very small in the land areas, even negative in the middle latitudes where condensation of air water vapor on the ground often happens, but large in the ocean areas. In July, however, the eastern United States has the largest evapotranspiration of about 200 mm. Evapotranspiration decreases toward the west and is below 60 mm in parts of the southwest. Evapotranspiration changes due to the restoration are positive for both months, with a much larger magnitude in July, 0·3 in January and 1·5 mm in July (Table I). The restoration should lead to a noticeable increase in evapotranspiration in the RR. However, precipitation is decreased in this region, which has an adverse contribution to evapotranspiration. Thus, only a small increase in evapotranspiration is found.

Present runoff has similar spatial patterns as precipitation, but with smaller magnitude (Figure 8). The change due to the forest restoration is mostly positive in

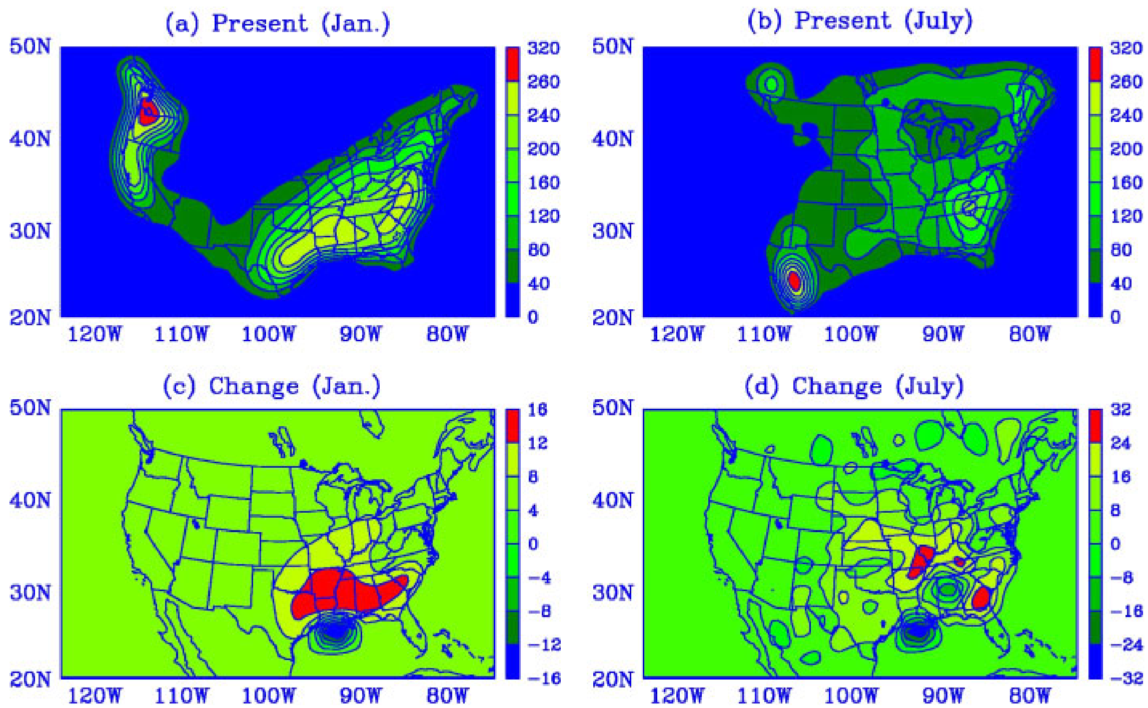

Figure 8. Runoff (mm/months) averaged over 8 years for present precipitation in January (a) and July (b), and change due to forest restoration in January (c) and July (d).

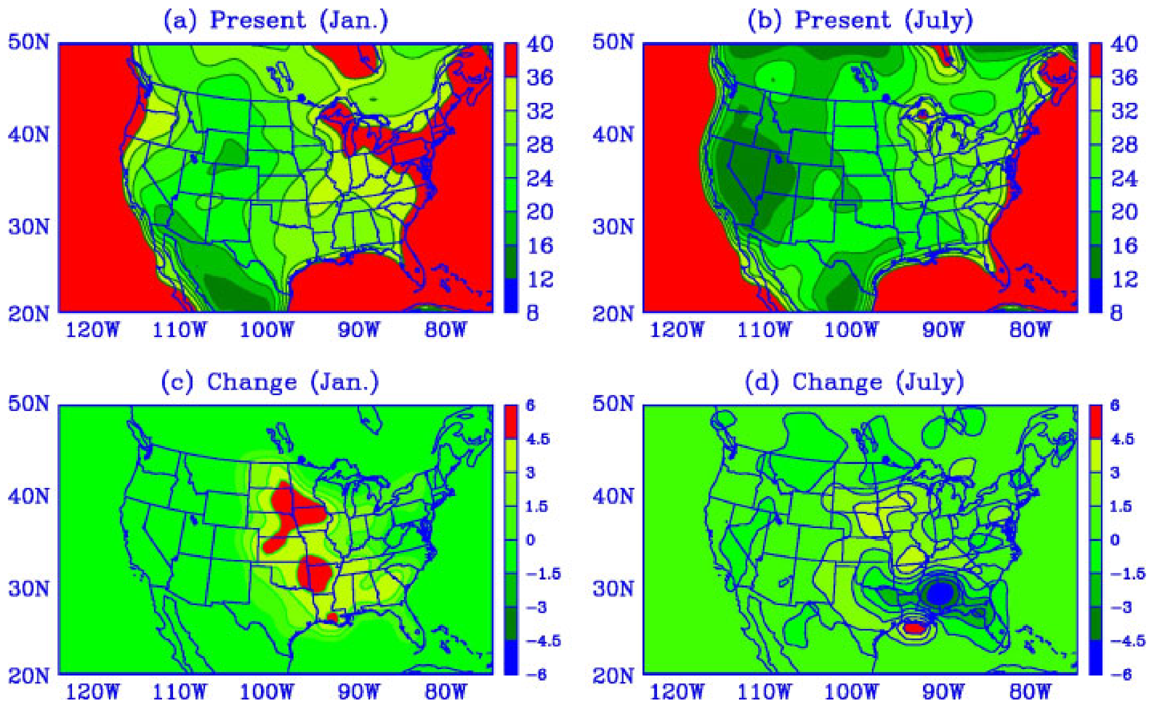

Figure 9. Surface-layer soil moisture (mm) averaged over 8 years for present precipitation in January (a) and July (b), and change due to forest restoration in January (c) and July (d).

January, and negative in July except in the Atlantic coast. The RR averages are 28 mm in January and 49 mm in July, and the corresponding changes due to the restoration are 5·6 and 7·7 mm, respectively (Table I). As described in the Section on Methods, runoff is proportional to precipitation in BATS (Dickinson *et al*., 1993), which was used to simulate land-surface hydrology in this study. Thus, precipitation is closely followed by runoff in both the simulated pattern and the change due to the forest restoration.

Soil moisture and air humidity. Soil moisture averages of the surface layer are higher in the eastern United States and lower in the western United States (Figure 9). The highest values are about 40 mm in the northeastern United States in January and about 30 mm in that

Table II. Water fluxes (mm/months) for the restoration region (RR), north (N), northwest (NW), west (W), south (S) and east (E) areas for soil moisture (mm) and air humidity (g/kg).

Area	Surface soil moisture		Root soil moisture		Air-specific humidity	
	January	July	January	July	January	July
RR	32 (2·4)	26 (−0·2)	548 (225)	525 (226)	5·0 (−0·02)	16·2 (−0·5)
N	35 (1·5)	29 (0·4)	428 (24)	413 (22)	2·5 (0·02)	14·0 (0·1)
NW	26 (2·6)	23 (0·8)	286 (32)	267 (31)	2·4 (0·04)	13·1 (0·5)
W	29 (1·5)	23 (0·5)	322 (28)	296 (27)	3·9 (0·06)	14·7 (0·3)
S					13·4(0·01)	21·5(0·02)
E					14·0 (0·0)	20·8 (0·01)

See Figure 4 for locations.

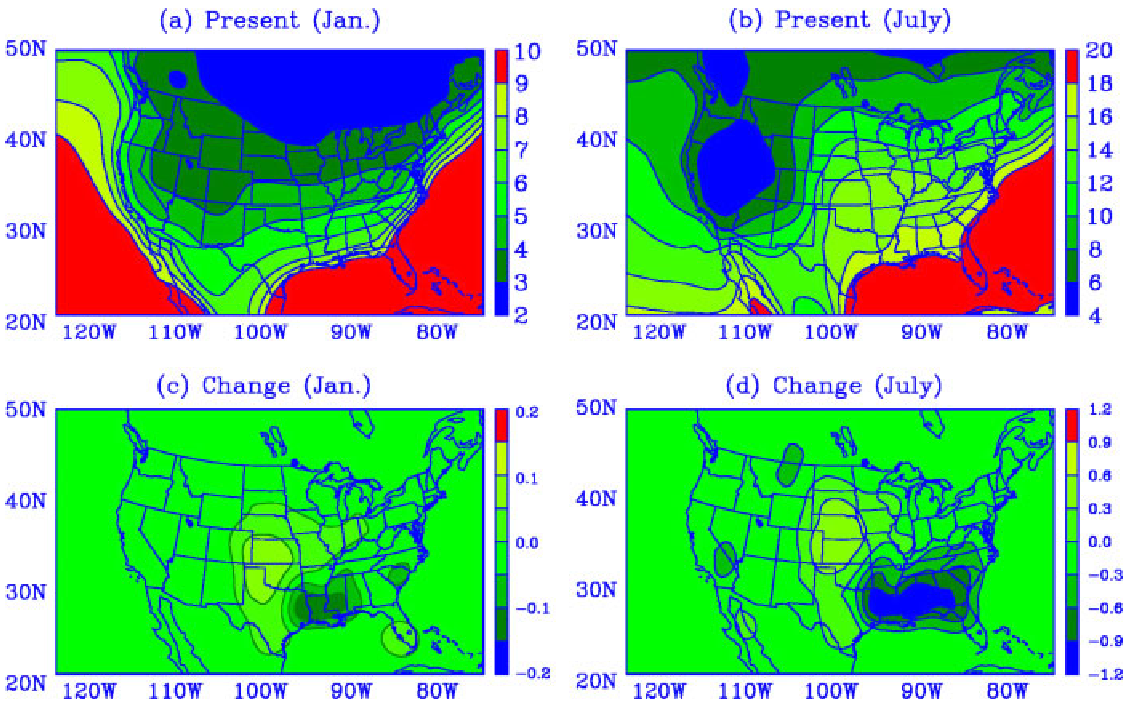

Figure 10. Air-specific humidity (g/kg) averaged over 8 years for present precipitation in January (a) and July (b), and change due to forest restoration in January (c) and July (d).

region and in the Atlantic coast in July. The lowest values are found in the Great Plains and central Rocky Mountains in January and inter-mountains in July. The forest restoration leads to soil moisture increase in January and slight decrease in July in the RR. The RR averages are 32 mm in January and 26 mm in July and the corresponding changes due to the restoration are 2·4 and −0·2 mm, respectively (Table II).

Soil moisture averages of root layer (figure not shown) are the highest in the Atlantic coast and lowest in the Pacific coast, with a magnitude of 600 and 200 mm, respectively. The changes due to restoration are significant mainly in the RR. The spatial patterns are similar between January and July. The RR averages and changes due to the restoration in January are 548 and 225 mm, respectively (Table II). There are only small differences in the magnitude between July and January.

The small difference in root-layer soil moisture between the 2 months is mainly related to the way of specifying initial soil moisture in the simulations and the nature of slow process in soil moisture variations. The initial soil moisture was specified based on soil type and land cover type, which are time independent. This means that there was no difference in initial soil moisture conditions between January and July. Surface soil layer responds more quickly to atmospheric conditions than root layer within the range allowed by their specific soil properties, because surface soils are in direct contact with overlying atmosphere.

Air humidity is determined mainly by latitude and the ground type. Air-specific humidity averages in January increase from below 2 g/kg in middle latitudes to 8 g/kg in the low-latitude land areas and further to over 10 g/kg in the ocean areas (Figure 10). There are two differences for July. First, a gradient with high moisture in the eastern United States and low moisture in the western United States is found. Second, air humidity magnitude in July is about twice as large as that in January. The spatial patterns in the change due to the restoration are similar between January and July.

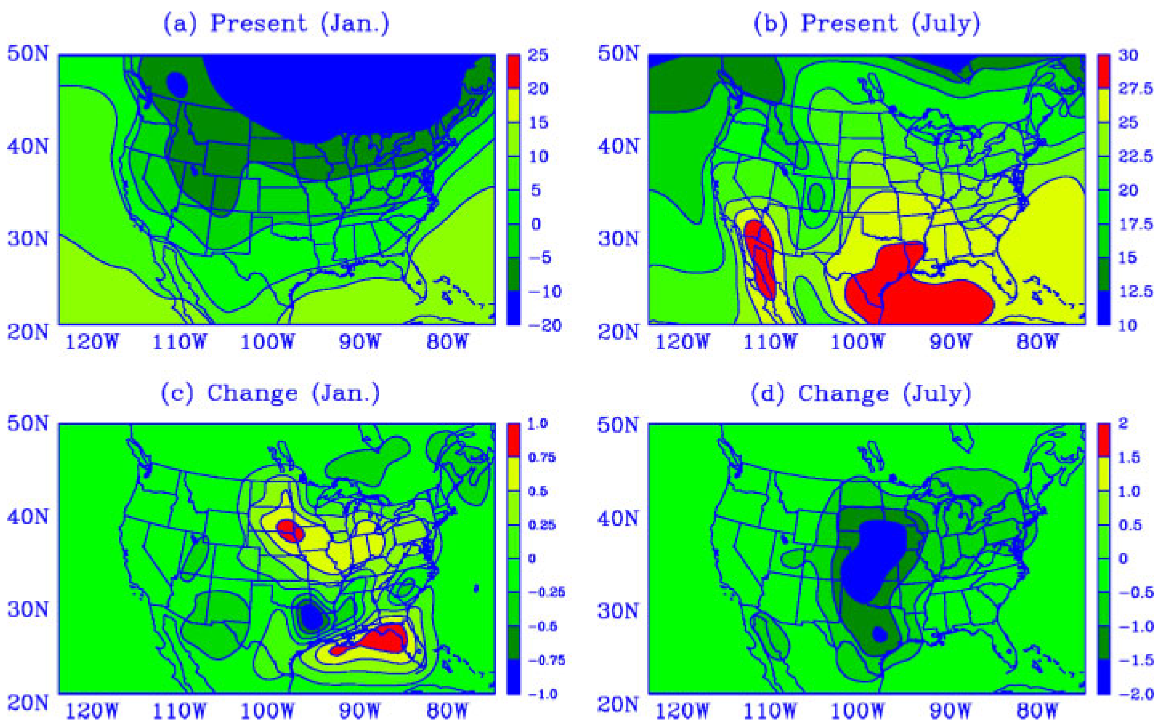

Figure 11. Air temperature (°C) averaged over 8 years for present precipitation in January (a) and July (b), and change due to forest restoration in January (c) and July (d).

Air-specific humidity decreases in the RR with a larger magnitude in July. The RR values are 5 g/kg in January and 16·2 g/kg in July and the corresponding changes due to the restoration are −0·02 and −0·5 g/kg, respectively (Table II).

Air temperature. The simulated air temperature near the ground shows a general trend of decrease from the low to middle latitudes in January (Figure 11). Temperature is lower over the inland than the coastal regions and the lowest over the Rocky Mountains. The July temperature shows the same latitudinal dependence, but the topographic effect is more significant. Two warm tongues (the areas with higher temperature than the surrounding areas) extend from Texas to the northern Great Plains and along the Pacific coast, separated by the Rocky Mountains where temperature is lower due to the high elevation. Temperature is lower in the Atlantic coast, where large rainfall is located, than in the central United States at the same latitudes, an indication of the effect of clouds and precipitation. The restoration leads to January temperature decreases in most of the RR and increases in the southern part of the region and the Midwest. July temperature is nearly unchanged in the RR but decreases in the central United States. The RR averages of air temperature are 4·7 °C in January and 26 °C in July. The corresponding changes are very small.

Surrounding areas

The restoration also leads to changes in the surrounding areas. January precipitation increases in all surrounding areas except N where the change is −1·0 mm (Table I). July precipitation decreases in S by −2·6 mm but increases in the other areas, by 4·7 mm in W and 9·8 mm in NW. January evapotranspiration increases in all land areas but decreases in the ocean ones. July evapotranspiration increases by 9·8 and 11·7 mm in NW and W, and changes little in the ocean areas. Runoff increases mostly in both January and July in the surrounding land areas, with the July values between 3·5 and 5·8 mm. Soil moisture increases (Table II) by 1·5–2·6 mm in the surface layer and 22–31 mm in the root layer in July. There is only a small difference in the magnitude between the 2 months. Air humidity increases mostly, by 0·02–0·06 g/kg in January and 0·5 g/kg in NW in July. Air temperature decreases by 0·43 °C in W in July (Table III).

Physical processes

The ground surface consists of vegetation and bare soil. Albedo is smaller on vegetated than on bare soil. If vegetated soil increases (thus bare soil decreases), the albedo of the ground surface will be reduced. As described in the conceptual model (Figure 1), when agricultural lands are replaced with forests, surface albedo is reduced and therefore more solar radiative energy is absorbed by the ground. Solar radiation in RR is 137 and 298 Wm^{-2} in January and July, respectively, and increases by 1·8 and 5·9 Wm^{-2} due to the restoration (Table IV). In January, nearly half the increased solar radiation, 0·8 Wm^{-2}, is converted into sensible heat, while a smaller amount, 0·3 Wm^{-2}, is converted into latent heat. The rest of the increased solar radiation is used to increase soil temperature. In July, nearly 75% of the increased solar radiation is used to increase sensible heat flux. The situation is different in the surrounding areas, especially in NW and W

Table III. Water fluxes (mm/months) for the restoration region (RR), north (N), northwest (NW), west (W), south (S) and east (E) areas for air temperature (°C) and winds (ms^{-1}).

	Air temperature		Westerly wind speed		Southerly wind speed	
	January	July	January	July	January	July
RR	4·7 (0·02)	26 (−0·01)	0·3 (−0·02)	0·4 (−0·32)	−0·02 (0·11)	0·83 (−0·55)
N	−5·5 (0·12)	22 (−0·2)	1·6 (0·0)	0·7 (−0·03)	0·6 (0·01)	0·6 (−0·08)
NW	−5·1 (0·11)	26 (−0·01)	2·6 (0·0)	0·0 (−0·04)	−1·0 (0·01)	0·8 (−0·6)
W	2·5 (0·02)	26 (−0·43)	0·9 (−0·01)	0·3 (−0·03)	−0·4 (−0·03)	1·6 (−0·01)
S	18·0 (0·13)	27 (0·0)	−2·2 (0·09)	−1·5(0·1)	−1·3 (0·11)	1·1 (−0·04)
E	28·5 (0·01)	26 (0·03)	0·8 (−0·02)	0·7 (0·02)	0·2 (−0·02)	2·6 (0·23)

See Figure 4 for locations.

Table IV. Water fluxes (mm/months) for the restoration region (RR), north (N), northwest (NW), west (W), south (S) and east (E) areas for energy fluxes (Wm^{-2}).

Area	Solar radiation		Sensible heat flux		Latent heat flux	
	January	July	January	July	January	July
RR	137 (1·8)	298 (5·9)	11 (0·8)	48 (4·3)	43 (0·3)	178 (1·4)
N	95 (0·3)	298 (0·1)	−1·0 (0·3)	31 (−1·8)	17 (0·3)	168 (3·0)
NW	94 (0·4)	294 (0·0)	−13 (0·0)	48 (−7·6)	14 (0·9)	159 (11·3)
W	131 (0·5)	292 (0·1)	3·5 (−0·7)	57 (−7·0)	34 (1·5)	158 (9·5)
S	179 (0·5)	323 (1·2)	38 (−2·7)	17 (−0·1)	143 (−3·3)	127 (−0·3)
E	161 (0·0)	332(−0·1)	57 (−0·2)	7 (−0·3)	203 (−0·5)	109 (11·3)

See Figure 4 for locations.

during July. There is little change in solar radiation due to the restoration. But sensible heat flux is reduced by 7·6 and 7·0 Wm^{-2}, while latent heat flux is increased by 11·3 and 9·5 Wm^{-2}, respectively, in the two areas. These changes are responsible for the temperature decreases there. The effects of the restoration on the surrounding areas are caused by the change in atmospheric circulation, as described below. Atmospheric circulation consists of systems at various spatial scales including those larger than the size of the restoration. An example is the anti-cyclonic system centered in the Atlantic Ocean. The effects could be more significant in some regions than other regions.

The causes for precipitation change, however, are very complex. There are three contributors to precipitation formation, i.e. atmospheric circulation dynamical systems, water vapor transport, and vertical thermal stability. Figure 12 shows the simulated air streamlines and their changes due to the forest restoration. The January streamlines are characterized by an anti-cyclonic circulation in the United States, representing a high-pressure system with cool and dry airflows. It has a center in the Southwest with two high-pressure ridge lines, along which air pressure is higher than outside. One line extends northward along the Rocky Mountains, responsible for very small precipitation in the central United States (Figure 5). The other line extends eastward along the Gulf coast. Between the two lines is the westerly trough in the eastern United States, a rain generator for this region. Parts of the circulation systems in the ocean areas can be seen in the simulation domain. A trough exists in the northern Pacific as part of the planetary westerly system, which brings large rainfall in the northwest Pacific coast. Each of the two oceans has a high pressure system in the subtropical area.

The RR is under the control of northerly cool and dry airflows in January. Because of the increased roughness with forest restoration, the prevailing wind speed is reduced, as indicated by the opposite direction in the change of streamlines to that of original streamlines. The westerly wind speed average in RR is 0·3 m s^{-1} (positive value indicates airflows from west to east). The speed decreases by 0·02 m s^{-1} due to the restoration (Table III). The southerly wind speed average is −0·02 m s^{-1} (positive value indicates airflows from south to north) and 0·11 m s^{-1} for change. The magnitude of changed wind speed is smaller than that of the average wind speed, indicating that the direction of the original airflows remains the same after the restoration, but only their speed is reduced. The exception is the southerly wind. A slight northerly wind turns to a southerly wind after the restoration. This change in northerly wind speed indicates that more water vapor is transported into the RR, which explains the increase in precipitation. Meanwhile, there are two well-developed circulation systems in the changed airflows in the surrounding areas. One is a cyclonic circulation located in Louisiana, Arkansas, and northeastern Texas, which is an atmospheric system to produce water vapor condensation. The other is an anti-cyclonic circulation located in the northern surrounding area, which is an atmospheric system to depress water vapor condensation.

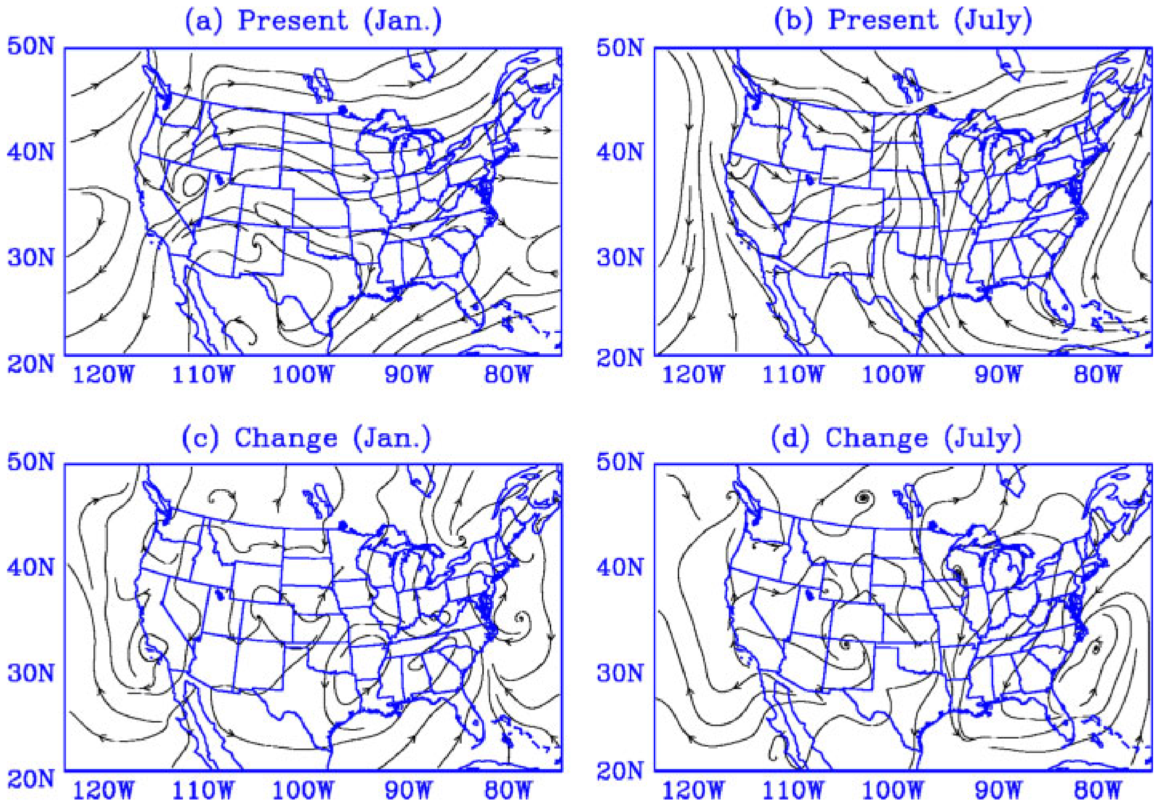

Figure 12. Airflow streamline on the ground averaged over 8 years for present precipitation in January (a) and July (b), and change due to forest restoration in January (c) and July (d).

They explain the mostly positive and negative rainfall changes in these two areas, respectively.

In July, the Atlantic high-pressure system advances northwestward into the land area, while the Pacific one moves up northward. Between them is an extensive low pressure system in the United States with two trough lines near the United States–Canada and United States–Mexico border areas, respectively. The lines generate large rainfall. Atmospheric systems at the planetary scale usually expand from the ground to the free atmosphere, but the core of each system tilts eastward with increased height. Because condensation of atmospheric water vapor happens mostly in the free atmosphere, the actual rainfall region is located more east than the location of a trough line near the ground.

The RR is under the control of warm and moist air in July. As in January, the prevailing wind speed is reduced. The westerly wind speed average in RR is 0·4 m s^{-1}, and decreases by 0·32 m s^{-1} due to the restoration (Table III). The corresponding average and change for southerly winds are 0·83 and −0·55 m s^{-1}, respectively. This change indicates less water vapor transported into the RR, explaining the decrease in precipitation. Although the forested areas transpire more water into the atmosphere, which should increase precipitation, the horizontal water vapor transport is reduced with the magnitude larger than that of the increase due to the change in transpiration. Thus, the combined effects of the water transports lead to a reduction in July precipitation in the RR. There is a well-developed cyclonic circulation in the Atlantic area in the changed airflows, responsible for the positive rainfall change there. On the other hand, the northerly winds in the changed airflows spread over the western surrounding area and there is an anti-cyclonic circulation in the Great Lakes area, responsible for the rainfall decrease in the two areas. Between the two areas is rainfall increase in the central Midwest.

The result of the July precipitation decrease from this study is opposite to the simulated precipitation change due to the afforestation in northern China. A forest shelterbelt project started in 1978 across dry northern China (SFA, 2006). The project aims to prevent southward expansion of the desert, improve hydroclimate conditions, and conserve the natural environment in the project region. The forest shelterbelt is about 7000 km long zonally and 400–1700 km wide. It stands along the southern edge of the sandy lands, nearly paralleling to the Great Wall. It was targeted to complete by 2050. A similar modeling study indicated overall precipitation increase due to the afforestation (Liu *et al*., 2008). The difference in precipitation change between the two regions is related to the difference in their atmospheric circulation systems. In contrast to the forest RR in the subtropical southeastern United States where the prevailing July winds are southerly, the afforestation region in the northern China is located in the middle latitudes with the westerly prevailing winds. The cool and dry winds are reduced due to the afforestation. In the south of the afforested region, meanwhile, the warm and moist southerly airflows from the subtropical Pacific

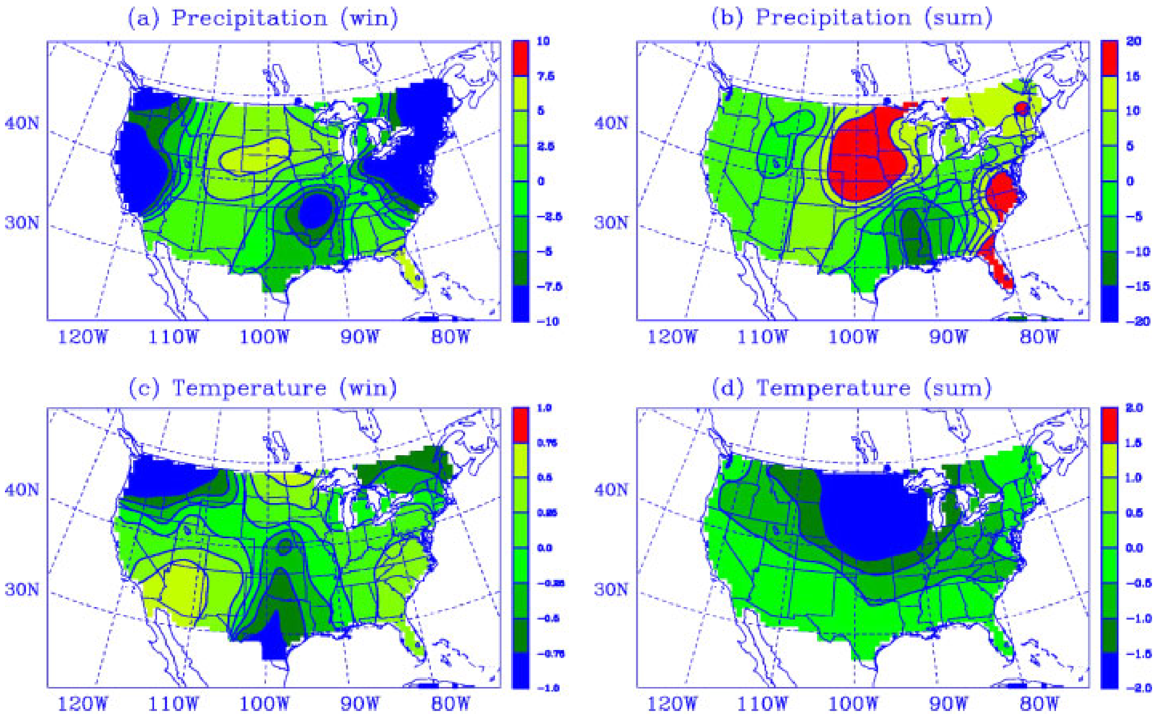

Figure 13. Differences of 10-year averages between 1940s and 1930s. Panels (a) and (b) are January and July precipitation, respectively (mm/months), and panels (c) and (d) are January and July air temperature, respectively (°C).

Ocean move closer to the afforested region, carrying more atmospheric water vapor and as a result, generating more precipitation.

Evaluation

The observed January precipitation increased in the eastern portion of the RR but decreased in the western portion from the 1930s to 1940s (Figure 13). Outside the region, it increased in the Midwest and the Southwest, but decreased along the Pacific coast and Mid-Atlantic coast. The observed July precipitation decreased in most of the RR except the Atlantic coast, increased in the Northeast, and changed little along the Pacific coast. The magnitude of the differences was about 10 and 20 mm per month in January and July, respectively. There are some major common features between the observed precipitation differences and the simulated changes due to the restoration, both being negative from the western Gulf coast to the Northeast and positive in the low-Atlantic coast in January, and negative in most of the RR except the Atlantic coast in July. No observed runoff data were compared with the simulated ones. However, it is expected that similar changes between runoff and precipitation occurred from the 1930s to 1940s because runoff was proportional to precipitation.

The spatial pattern of the observed January air temperature difference from the 1930s to 1940s was similar to that of precipitation, with cooling corresponding to drying. The pattern in July was characterized by little change in the RR and large cooling in the Midwest, which is similar to a certain extent to that of the simulated changes due to the restoration, especially in July,

Sun *et al.* (2010) conducted a measurement study to compare energy and water balance between a pair of forested and clearcut sites in North Carolina. Despite many differences in geographic locations and times between the measurement and this simulation, their findings support simulation assumptions and results that forest canopy had a lower albedo, received more solar radiation, higher latent heat flux, and small difference in air temperature. The measurement indicated that the forest site had smaller runoff. The changes in the simulated runoff due to the restoration show significant spatial variability. It is reduced in a large portion of the RR in July, but slightly increased along the Atlantic coast where the experimental measurements were conducted, responding to the increase in the simulated precipitation. The measurements revealed the impacts of forested cover on local microclimate and hydrological properties. The RR in this simulation, on the other hand, covers a large portion of the South. The simulation reveals the changes due to both local and large-scale processes. Those related to the large-scale processes could be location dependent, as seen from the differences in precipitation and other water fluxes between the Atlantic coast and the western portion of the RR. This spatial variability creates difficulty in comparisons between the measured and simulated results.

CONCLUDING REMARKS

Significant impacts of the forest restoration in the southern United States on hydrology have been obtained from numerical simulations and experiments with the RegCM. Precipitation mostly decreases in July and increases in

January due to the restoration. This change is mainly caused by the reduction in the prevailing winds due to increased surface roughness. The reduction in southerly winds in July means weaker moist transport and therefore smaller precipitation. In contrast, the reduction in the northerly winds in January means weaker dry and cold airflows and therefore more precipitation. The difference in July prevailing winds between the southern United States and northern China is also the main cause for opposite precipitation changes induced by afforestation in the two regions. There is inter-annual variability with precipitation change. Among the 8 years, July precipitation is overall decreased in 5 years, decreased but with small magnitude in 2 years, and increased in 1 year. The impacts on other hydrological properties in the RR are mostly related to the changes in local vegetation and soil properties. Forest restoration brings larger vegetation coverage and larger transpiration, leading to larger evapotranspiration. Soil moisture of root layer is increased.

The impacts on precipitation of the restoration can go beyond the restored region through the change in the atmospheric circulation. This change is responsible for a large increase in precipitation in the central Midwest as well as the western and northern surrounding areas. This further leads to large changes in other hydrological and climatic conditions, including increases in evapotranspiration (latent heat flux), runoff, soil moisture, and air specific humidity, and decreases in sensible heat flux.

The projected future vegetation change from the temperate deciduous forests to temperate deciduous savanna in a large portion of the Southeast due to the greenhouse effect (Neilson *et al*., 1998, 2005) is opposite to the forest conversion investigated in this study. Thus, opposite impacts on hydrology and climate are expected for the projected vegetation change. On the other hand, the project to replace pasture and farming lands with trees in the Southeast, Great Lake states, and the Corn Belt states (Watson, 2009) will affect hydrological and climate conditions in these regions. The results from this study suggest that the afforestation project would not only change hydrological conditions in the planting areas, but also their surroundings. It is important to assess both local and remote impacts and make a comprehensive plan to achieve best hydrological benefits in the entire United States In addition, when selecting planting areas for the large-scale silviculture, attention should be paid to these regions where vegetation conditions are projected to change significantly under the changing climate. For the non-forest areas at present that are projected to become forests in the future, there might be no need for silviculture. For the forest areas at present that are projected to become savanna, planting could be made, but caution is needed to select those species that can survive the future drier climate conditions.

Some efforts have been made in this study to evaluate the simulation results with the historical meteorological data and hydrological measurements. More evaluations, however, are needed. This is a challenge because of the lack of soil hydrologic measurements across the afforestation region. In addition, the simulation period in this study is much shorter than the actual forest restoration process, and historical meteorological conditions during the forest restoration period were not used in the simulation. The next effort toward improving this numerical study is to conduct long-term simulations using actual initial and boundary meteorological conditions. Ideally, dynamical vegetation models are coupled with climate models to reproduce the growth of planted trees during the restoration.

ACKNOWLEDGMENTS

The author thanks the thoughtful and constructive comments from the reviewers and editor. This study was supported by the USDA Forest Service. The meteorological data for driving the regional climate model were obtained from the National Center for Atmospheric Research.

REFERENCES

Allen AW, Bernal YK, Moulton RJ. 1996. *Pine plantations and wildlife in the southeastern United States: an assessment of impacts and opportunities*. Information and Technology Report 3. US Department of the Interior, National Biological Service; 32. www.nwrc.usgs.gov/wdb/pub/others/1996_03.pdf.

Andersen OB, Seneviratne SI, Hinderer J and Viterbo P. 2005. GRACE-derived terrestrial water storage depletion associated with the 2003 European heat wave. *Geophysical Research Letter* **32**: L18405.

Anthes RA, Hsie E-Y, Kuo Y-H. 1987. *Description of the Penn State/NCAR Mesoscale model version 4 (MM4)*. Technical Note, NCAR/TN-282+STR. National Center for Atmospheric Research: Boulder, Colorado; 66.

Bonan GB. 1997. Effects of land use on the climate of the United States. *Climatic Change* **37**: 449–486.

Caya D, Laprise R. 1999. A semi-implicit semi-lagrangian regional climate model: the Canadian RCM. *Monthly Weather Review* **127**: 341–362.

Dickinson RE Durbudge TB Kennedy PJ McGuffie K Pitman AJ. 1993. Tropical deforestation: modeling local- to regional-scale climate change *Journal of Geophysical Research* **98**(D4): 7289–7315.

Dickinson RE, Errico RM, Giorgi F, Bates GT. 1989. A regional climate model for the western U.S. *Climatic Change* **15**: 383–422.

Dickinson RE, Henderson-Sellers A, Kennedy PJ. 1995. *Biosphere-atmosphere transfer scheme (BATS) version 1E as coupled to the NCAR community climate model*. NCAR Tech. Note/TN-387. NCAR: Boulder, CO; 72.

Dickinson RE, Kennedy P. 1992. Impacts on regional climate of Amazon deforestation. *Geophysical Research Letters* **19**: 1947–1950.

Giorgi F, Bates GT. 1989. The climatological skill of a regional model over complex terrain. *Monthly Weather Review* **117**: 2325–2347.

Giorgi F, Bi X. 2000. A study of internal variability of a regional climate model. *Journal of Geophysical Research* **105**: 29503–29521.

Giorgi F, Marinucci MR, De Canio G, Bates GT. 1993a. Development of a second generation regional climate model (RegCM2), I, Boundary layer and radiative transfer processes. *Monthly Weather Review* **121**: 2794–2813.

Giorgi F, Marinucci MR, De Canio G, Bates GT. 1993b. Development of a second generation regional climate model (RegCM2), II, convective processes and assimilation of lateral boundary conditions. *Monthly Weather Review* **121**: 2814–2832.

Giorgi F, Shields C. 1999. Tests of precipitation parameterizations available in latest version of NCAR regional climate model (RegCM) over continental United States. *Journal of Geophysical Research* **104**: 6353–6375.

Grell GA, Dudhia J, Stauffer DR. 1994. A description of the fifth generation Penn State/NCAR mesoscale model (MM5), NCAR/TN-398+STR. National Centre for Atmospheric Research: Boulder, CO; 122.

Henderson-Sellers A, McGuffie K. 1995. Global climate models and 'dynamic' vegetation changes. *Global Change Biology* **1**: 63–75.

IPCC (Intergovernmental Panel on Climate Change). 2007. *Climate change 2007*. Cambridge University Press, 1056 pp.

Jackson R, Jobbagy BEG, Avissar R, Roy SB, Barrett DJ, Cook CW, Farley KA, le Maitre DC, McCarl BA, Murray BC. 2005. Trading water for carbon with biological carbon sequestration. *Science* **310**: 1944–1947.

Jones RG, Murphy JM, Noguer M. 1995. Simulation of climate change over Europe using a nested regional-climate model. I: assessment of control climate, including sensitivity to location of lateral boundaries. *Quarterly Journal of the Royal Meteorological Society* **121**: 1413–1449.

Juang H-MH, Kanamitsu M. 1994. The NMC nested regional spectral model. *Monthly Weather Review* **122**: 3–26.

Kiehl JT, Hack JJ, Bonan GB, Boville BA, Briegleb BP, Williamson DL, Rash PJ. 1996. *Description of the NCAR community climate model (CCM3)*. NCAR/TN-420+STR. National Center for Atmospheric Research: Boulder, CO.

Lean J, Warrilow DA. 1989. Simulation of the regional climatic impact of Amazon deforestation. *Nature* **342**: 411–413.

Liang X-Z, Pan J, Zhu J, Kunkel KE, Wang JXL, Dai A. 2006. Regional climate model downscaling of the U.S. summer climate and future change. *Journal of Geophysical Research* **111**: D10108, DOI:10.1029/2005JD006685.

Liston GE, Pielke RA Sr. 2000. A climate version of the regional atmospheric modeling system. *Theoretical and Applied Climatology* **66**: 29–47.

Liu Y-Q. 2005. Enhancement of the 1988 Northern U.S. drought due to wildfires. *Geophysical Research Letters* **32**(10): L1080610.1029/2005GL022411.

Liu Y-Q. 2007. Advances in regional climate modeling. In *Proceedings of Int'l Symposium on Advances in Atmospheric Science and Information Technology*. Nanjing, China; 94–100.

Liu Y-Q, Liu S-C, Dickinson RE. 2000. Regional response of atmospheric circulation and surface energy and water balance to observed distribution of aerosol loading over the United States. *Abstracts of Seventh International Conference on Atmospheric Sciences and Applications to Air Quality*. Taipai, Taiwan. 178.

Liu Y-Q, Stanturf J, Lu H. 2008. Modeling the potential of the Northern China forest shelterbelt in improving hydroclimate conditions. *Journal of the American Water Resources Association* **44**(5): 1176–1192.

Liu Y-Q, Stanturf J, Goodrick S. 2010a. Trends in global wildfire potential in a changing climate. *Forest Ecology and Management*, **259**: 685–697, DOI:10.1016/j.foreco.2009.

Liu Y-Q, Stanturf J, Goodrick S. 2010b. Wildfire potential evaluation during a drought event with a regional climate model. *Ecological Informatics* (in press).

McVicar TR, Li LT, Niel TGV, Zhang L, Li R, Yang QK, Zhang XP, Mu XM, Wen ZM, Liu WZ, Zhao YA, Liu ZH, Gao P. 2007. Developing a decision support tool for China's re-vegetation program: simulating regional impacts of afforestation on average annual streamflow in the Loess Plateau. *Forest Ecology and Management* **251**: 65–81.

Neilson RP, Pitelka LF, Solomon A, Nathan R, Midgley GF, Fragoso J, Lischke H, Thompson K. 2005. Forecasting regional to global plant migration in response to climate change: challenges and directions. *BioScience* **55**: 749–759.

Neilson RP, Prentice IC, Smith B, Kittel TGF, Viner D. 1998. Simulated changes in vegetation distribution under global warming. In *The Regional Impacts of Climate Change: An Assessment of Vulnerability*, Watson RT, Zinyowera MC, Moss RH, Dokken DJ (eds). Cambridge University Press: Cambridge, United Kingdom; 439–456.

Nobre CA, Sellers PJ, Shukla J. 1991. Amazonian deforestation and regional climate change. *Journal of Climate* **4**: 957–988.

Pielke RA, Avissar R. 1990. Influence of landscape structure on local and regional climate. *Landscape Ecology* **4**: 133–155.

Sampson RN. 2004. Southern forests: yesterday, today, and tomorrow. In *Southern Forest Science: Past, Present, and Future*, Michael Rauscher H, Johnson Kurt (eds). Department of Agriculture Forest Service: General Technical Report SRS-75; 408.

Seth A, Giorgi F. 1998. The effects of domain choice on summer precipitation simulation and sensitivity in a regional climate model. *Journal of Climate* **11**: 2698–2712.

SFA (China State Forest Administration). 2006. *China's forest shelter project dubbed "green Great Wall"*, www.chinaview.cn. accessed 09 July 2006.

Shea DJ, Trenberth KE, Reynolds RW. 1992. Global monthly sea surface temperature climatology. *Journal of Climate* **5**: 987–1001.

Shukla J, Nobre CA, Sellers PJ. 1990. Amazonia deforestation and climate change. *Science* **247**: 1322–1325.

SRFRR. 1996. Southern region forest research report. *7th American Forest Congress, Feb. 1996*. Washington, DC, USA.

Stanturf JA, Gardiner ES, Hamel PB, Devall MS, Leininger TD, Warren ME. 2000. Restoring bottomland hardwood ecosystems in the Lower Mississippi Alluvial Valley. *Journal of Forestry* **98**: 10–16.

Sun G, Noormets A, Gavazzi1 MJ, McNulty SG, Chen J, Domec J-C, King JS, Amatya DM, Skaggs RW. 2010. Energy and water Balance of two contrasting Loblolly pine plantations on the lower coastal plain of North Carolina, USA. *Forest Ecology and Management* DOI:10.1016/j.foreco.2009.09.016.

Sun G, Zhou GY, Zhang ZQ, Wei XH, McNulty SG, Vose JM. 2006. Potential Water Yield Reduction Due to Forestation Across China. *Journal of Hydrology* **328**: 548–558.

USDAFS (U.S. Department of Agriculture, Forest Service), 1994. *Pest and pesticide management on southern forests*. Manage. Bull. R8–MB 60. U.S. Department of Agriculture, Forest Service, Southern Region: Atlanta.

USDA (U.S. Department of Agriculture), 1988. The south's fourth forest: Alternatives for the future. U.S. Forest Service Resource Report 24. Washington, D.C. 5I2 pp.

Watson T. 2009. *Climate plan calls for forest expansion*, USA TODAY. www.usatoday.com/news/nation/environment/2009-08-19-forest_N.htm. Accessed date is August 19, 2009.

Xue YK. 1996. The impacts of desertification in the Mongolian and the Inner Mongolian grassland on the regional climate. *Journal of Climate* **9**: 2173–2189.

Zeng X, Dickinson RE, Walker A, Shaikh M, DeFries RS, Qi J. 2000. Derivation and evaluation of global 1-km fractional vegetation cover data for land modeling. *Journal of Applied Meteorology* **39**: 826–839.